High-performance quantum ring detector for the 1–3 terahertz range

S. Bhowmick, G. Huang, W. Guo, C. S. Lee, P. Bhattacharya et al.

Citation: Appl. Phys. Lett. **96**, 231103 (2010); doi: 10.1063/1.3447364
View online: http://dx.doi.org/10.1063/1.3447364
View Table of Contents: http://apl.aip.org/resource/1/APPLAB/v96/i23
Published by the American Institute of Physics.

High-performance quantum ring detector for the 1–3 terahertz range

S. Bhowmick,[1,a)] G. Huang,[1] W. Guo,[1] C. S. Lee,[1] P. Bhattacharya,[1] G. Ariyawansa,[2] and A. G. U. Perera[2]
[1]*Department of Electrical Engineering and Computer Science, Solid State Electronics Laboratory, University of Michigan, Ann Arbor, Michigan 48109-2122, USA*
[2]*Department of Physics and Astronomy, Georgia State University, Atlanta, Georgia 30303, USA*

(Received 25 February 2010; accepted 6 May 2010; published online 7 June 2010)

Molecular beam epitaxy of InAs/GaAs quantum dots and their subsequent transformation to quantum rings by postepitaxy thermal annealing have been investigated. Photoconductive detectors with multiple quantum ring layers in the active region exhibit dark current density $\sim 10^{-8}$ A/cm^2 at a bias of 2 V at 4.2 K. The rings have a single bound state, and emission of photoexcited carriers gives rise to a spectral response peaking at 1.82 THz (165 μm) at 5.2 K. Peak responsivity of 25 A/W, specific detectivity, D*, of 1×10^{16} Jones and a total quantum efficiency of 19% are measured with 1 V bias at 5.2 K. At 10 K and 1 V, D$^*\sim 3\times 10^{15}$ Jones is measured. © *2010 American Institute of Physics*. [doi:10.1063/1.3447364]

High performance terahertz (THz) detectors are in demand for astronomy and space applications.[1] For applications such as stand-off detection of plastic explosives,[2] it is important to detect radiation of frequency in the 1–3 THz range. Bolometers or extrinsic photodetectors, based on Ge, Si, or InSb, operated at 4.2 K or lower temperatures are currently used but their response is slow. Hence, the development of semiconductor based THz detectors,[3,4] whose operation is based on electronic transitions and having figures of merit comparable to those of bolometers, will have an appeal due to their high speed even if they operate at low temperatures.

Semiconductor-based quantum dot (QD) intersublevel detectors[5–9] have been used for the detection of infrared radiation in the 1–30 μm range. Quantum rings (QRs) are derived from epitaxially grown self-organized QDs by postgrowth annealing[10,11] and confinement in these nanostructures is stronger than that in dots because of the altered shape.[12] Detection up to 5 THz was recently demonstrated by us using QRs.[13] In the present study, we have investigated the epitaxy and characteristics of smaller QRs, compared to those in Ref. 13, and of intersublevel THz photoconductive detectors with QR active regions. It is found that the quantum ring intersublevel detectors (QRIDs) exhibit very low dark current and strong response in the 1–3 THz range, with the peak response measured at 1.82 THz (165 μm) in the temperature range of 5–10 K. This detection peak is characterized by a peak responsivity of 25 A/W and specific detectivity of 1×10^{16} Jones. These characteristics compare very favorably with those of bolometers.

In order to get an estimate of the size of the QRs in which the intersublevel spacing would be in the 1–3 THz range, we have performed calculations using a simplified model. From atomic force microscopy (AFM) images such as one shown in Fig. 1(a), it is evident that the rings have a height in the range of 1.2–1.5 nm and inner and outer radii of 25 nm and 40 nm, respectively. Carrier confinement in the rings primarily results from their width and height. We have therefore, approximated the ring by a quantum wire of width and height equal to those of the QR (height of 1.2–1.5 nm and width of 15 nm) and solved the three dimensional Schrodinger equation using appropriate boundary conditions. The eigen energies of the matrix Hamiltonian are then calculated. With the dimensions considered, there is only one bound state in the potential well and Fig. 1(b) shows the energy positions of this state, which is also the ground state. It is

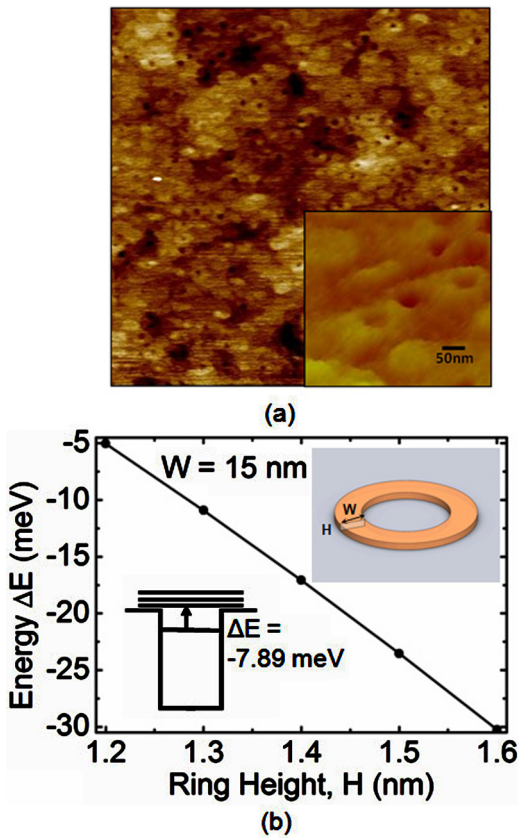

FIG. 1. (Color online) (a) AFM image of InAs QRs formed by postepitaxy thermal annealing of QDs. Inset shows a magnified image and dimensions; (b) calculated ground state energy in the QR as a function of ring height for ring width W=15 nm. Inset shows the schematic of the QR and calculated bound state in a QR with W=15 nm and H=1.25 nm. The transition energy of 7.89 meV corresponds to 1.91 THz.

a)Electronic mail: sishir@umich.edu.

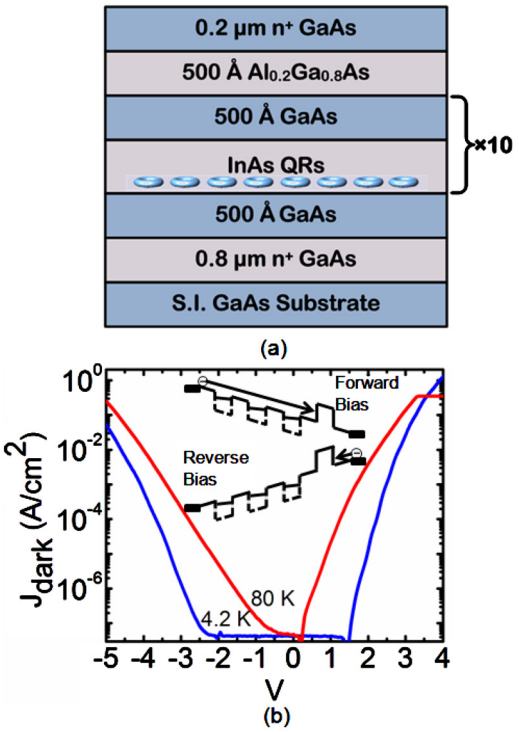

FIG. 2. (Color online) (a) Heterostructure schematic of QRID grown by MBE. It has ten layers of InAs QRs in the active region and a single $Al_{0.2}Ga_{0.8}As$ barrier at the end; (b) dark current characteristics at two different temperatures (4.2 and 80 K). Inset shows the conduction band profiles in the active region for forward and reverse bias.

evident that for QR height of 1.2–1.5 nm and width of 15 nm, the transition energy from the ground state to the continuum in the ring corresponds to the frequency range of 1–3 THz. It is important to note that the single confined state in the QR can be obtained only if they are made small. It may also be noted that we have used a simplified model for this calculation. In reality, the picture is more complex due to the actual shape of the ring and wave function overlap.

The QR ensembles and photoconductive detectors containing multiple QR layers were grown by molecular beam epitaxy (MBE) on semi-insulating (001) GaAs substrates. The growth parameters for the initial InAs QDs and the anneal conditions to convert them to QRs were initially investigated and carefully tuned to produce the desired smaller size of these nanostructures. For these experiments, a 0.8 μm GaAs buffer layer was first grown at 600 °C. The substrate temperature was then lowered to 530 °C and 2.1 monolayers of InAs were deposited at a rate of 0.08 monolayer/s. Self-organized QDs were formed following growth of 1.8 monolayers of InAs wetting layer. A 10 Å AlAs cap layer was grown on the InAs islands at 530 °C. Growth was interrupted and the capped islands were annealed at 580 °C for 30 s under an As_2 flux to form QRs. The function of the AlAs layer was to reduce the surface mobility of group III atoms on the AlAs surface, since AlAs has a higher bonding strength than GaAs. Consequently, the ring shape is better preserved during the annealing process. Under these growth conditions, small QRs as shown in the AFM image of Fig. 1(a) are obtained. The density of the rings is the same as the dots, which is $\sim 10^{10}$ cm^{-2}. The complete detector heterostructure, as shown in Fig. 2(a), is grown on (001) semi-insulating GaAs substrate with the ten QR layers grown and formed under the conditions described above. The 50 nm GaAs barrier layers shown in this figure are grown immediately after the formation of the QRs. A single $Al_{0.2}Ga_{0.8}As$ barrier is inserted at the end to reduce the dark current without substantially affecting the photocurrent.[14] The band profiles of the heterostructure for forward and reverse bias are shown in the inset of Fig. 2(b). Mesa shaped devices for top illumination were fabricated by photolithography, wet chemical etching, and n-contact metallization. The ring-shaped top contact has an inner radius of 300 μm, which defines the illumination area.

The QRIDs were characterized at cryogenic temperatures by dark current-voltage (I-V), spectral response, and noise measurements. The devices were inserted in a variable temperature liquid He cryostat for I-V measurements, which was done using a Keithley 2400 source meter. In order to determine the spectral responsivity of the detectors, the spectral response of the device under test and a Si composite bolometer with a sensitivity of 3×10^5 V/W were measured with a Perkin Elmer System 2000 Fourier transform infrared spectrometer. The two spectra were recorded with the same combination of optical windows, beam-splitter, and filters, so that the optical path is identical. A glow-bar was used as the radiation source. In order to confirm that the detection is not due to short wavelength (<62 μm) radiation, as in an optical pumping situation, a 62 μm cut-on filter was placed in front of the detector and the same detector response (but with reduced intensity due to the low transmission coefficient of the filter) was obtained. The voltage responsivity in V/W of the detectors was calculated by, $R=GSI_d/I_b$, where I_d is the raw detector spectrum, I_b is the bolometer raw spectrum, S is the bolometer sensitivity, and G is a geometrical factor which corrects for differences in the radiation-incident-area of the detector and the bolometer. To obtain the current responsivity in A/W, the voltage responsivity was divided by the effective resistance, which is the parallel combination of the load resistance R_l and the detector dynamic resistance $R_d(=dV/dI)$. The specific detectivity of the detectors at different temperatures and applied biases was obtained from, $D^*=R_p\sqrt{A}/\sqrt{S_i}$ where R_p is the measured peak responsivity, S_i is the noise current density, and A is the illuminated area of the detector. The noise current density was measured with a dual channel fast Fourier transform signal analyzer and a SR570 low noise current preamplifier.

The measured dark current densities at 4.2 and 80 K are shown in Fig. 2(b). The asymmetry in the I-V curves is due to the asymmetric structure of the device and can be understood in terms of the conduction band profiles shown in the inset. It may be noted that the dark current densities are extremely low; at T=4.2 K, $J=10^{-8}$ A/cm^2 and 10^{-6} A/cm^2 for bias of −2 V and +2 V, respectively. At T=80 K, $J=10^{-5}$ A/cm^2 and 10^{-3} A/cm^2 for bias of −2 V and +2 V, respectively.

The calibrated spectral response of the QRIDs at different biases and temperatures are shown in Figs. 3(a) and 3(b). There are several important points to be noted in the data. The responsivity peak at 1.82 THz (165 μm) corresponds to an energy of 7.52 meV, which agrees with the calculated ground state-to-continuum transition energy shown in Fig. 1(b) for the ring height of 1.25 nm. The observed full width at half maximum for the response peak at 165 μm is ~4.6 meV which is mainly attributed to the inhomogeneous

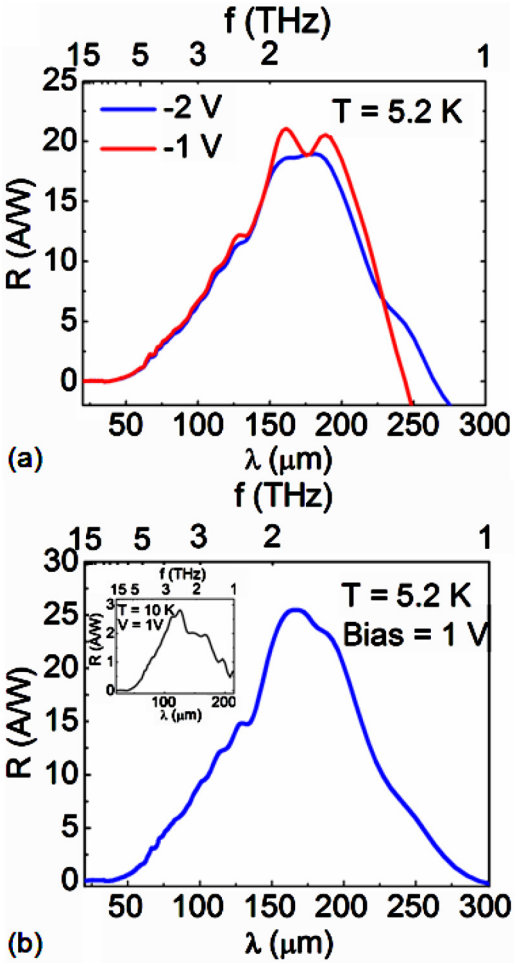

FIG. 3. (Color online) Measured spectral responsivity of QRID for (a) different reverse biases measured at 5.2 K, and (b) 1 V bias measured at 5.2 K. The inset to (b) shows the responsivity at 10 K under 1 V bias.

size distribution of the QRs. The multiple peaks in the data result from the measurement system. The observed high peak value of the responsivity $R_p \sim 20$ or 25 A/W, depending on bias polarity is due to the fact that the number of photons per 1 W of power at long wavelengths is higher compared to that in short wavelengths. The total quantum efficiencies (internal quantum efficiency × gain) are ~15 and 19% at −1 V and 1 V bias values, respectively. The $Al_{0.2}Ga_{0.8}As$ barrier layer with a height of 150 meV (assumed to be equal to the conduction band offset), do not seem to impede the transport and collection of photogenerated carriers under forward bias operation. The peak responsivity is larger under the forward bias than under the same amount of reverse bias (1 V). It may be noted that the trend of the dark current is also the same. We believe that the dark current contributes to the filling of bound states in the QR with electrons which eventually contribute to the photocurrent and responsivity. Hence, the trend in peak responsivity follows that of the dark current for opposite bias polarities. From Fig. 3(b) it is evident that the responsivity decreases sharply with increase in temperature from 5.2 to 10 K. In fact, at 12 K, the spectral response is too weak to measure. Due to the small energy difference between the bound state and the continuum in the QRs, any increase in temperature leads to emptying of electrons from the bound states to the states in the continuum. This also explains the shift of the responsivity peak to a higher energy (by 2.6 meV) when the measurement temperature is increased from 5.2 to 10 K [Fig. 3(b)]. The values of specific detectivity D^*, at a bias of 1 V, derived from the measured peak responsivity and noise current, are 1×10^{16} Jones and 3×10^{15} Jones at 5.2 K and 10 K, respectively. The chip had four circular mesas of 600 μm diameter and the data described above which represent several measurements at different times, is extremely consistent.

It is worthwhile to compare the measured characteristics of the QRIDs with those of bolometers that are currently used. The spectral response of the bolometers is generally uniform (flat) and their specific detectivity D^* is almost insensitive to temperature. The theoretical limit of D^* of bolometers is $\sim 10^{14}$ Jones at 10 K.[15] In contrast, the QRIDs reported here exhibit a response peak at 1.82 THz, which can be tuned by varying the size of the QRs. The specific detectivity is $\sim 10^{15}$ Jones, at 10 K, and higher at 5.2 K. The response time of the QRIDs, which is dependent on the emission and transport of the photoexcited carriers, is ~300 ps.[16] It seems that the present device cannot be operated at temperatures higher than 12 K due to thermal emission of electrons from the bound state to the continuum. We are currently investigating this aspect and device designs for higher temperature operation.

The work is supported by the Air Force Office of Scientific Research under Grant No. FA9550-09-1-0635 and STTR under Contract No. FA9550-09-C-0106, and the Georgia Research Alliance under Grant GRAUP.

[1] Y. C. Shen, T. Lo, P. F. Taday, B. E. Cole, W. R. Tribe, and M. C. Kemp, Appl. Phys. Lett. **86**, 241116 (2005).
[2] C. Baker, T. Lo, W. R. Tribe, B. E. Cole, M. R. Hogbin, and M. C. Kemp, Proc. IEEE **95**, 1559 (2007).
[3] M. B. M. Rinzan, A. G. U. Perera, S. G. Matsik, H. C. Liu, Z. R. Wasilewski, and M. Buchanan, Appl. Phys. Lett. **86**, 071112 (2005).
[4] H. Luo, H. C. Liu, C. Y. Song, and Z. R. Wasilewski, Appl. Phys. Lett. **86**, 231103 (2005).
[5] D. Pan, E. Towe, and S. Kennerly, Appl. Phys. Lett. **73**, 1937 (1998).
[6] S. Krishna, S. Raghavan, G. Winckel, A. Stintz, G. Ariyawansa, S. G. Matsik, and A. G. U. Perera, Appl. Phys. Lett. **83**, 2745 (2003).
[7] J. C. Campbell and A. Madhukar, Proc. IEEE **95**, 1815 (2007).
[8] G. Huang, J. Yang, P. Bhattacharya, G. Ariyawansa, and A. G. U. Perera, Appl. Phys. Lett. **92**, 011117 (2008).
[9] A. G. U. Perera, G. Ariyawansa, G. Huang, and P. Bhattacharya, Infrared Phys. Technol. **52**, 252 (2009).
[10] A. Lorke, R. J. Luyken, J. M. Garcia, and P. M. Petroff, Jpn. J. Appl. Phys., Part 1 **40**, 1857 (2001).
[11] D. Granados and J. M. Garcia, Appl. Phys. Lett. **82**, 2401 (2003).
[12] J. M. García, T. Mankad, P. O. Holtz, P. J. Wellman, and P. M. Petroff, Appl. Phys. Lett. **72**, 3172 (1998).
[13] G. Huang, W. Guo, P. Bhattacharya, G. Ariyawansa, and A. G. U. Perera, Appl. Phys. Lett. **94**, 101115 (2009).
[14] A. D. Stiff, S. Krisna, P. Bhattacharya, and S. W. Kennerly, IEEE J. Quantum Electron. **37**, 1412 (2001).
[15] R. Ciupa and A. Rogalski, Opto-Electron. Rev. **5**, 257 (1997).
[16] C. H. Lin, H. S. Lin, C. C. Huang, S. K. Su, S. D. Lin, K. W. Sun, C. P. Lee, Y. K. Liu, M. D. Yang, and J. L. Shen, Appl. Phys. Lett. **94**, 183101 (2009).